Compact Dual-Wideband Bandpass Filter Using a Novel Multiple-Mode Resonator

Jin Xu

College of Electronic Information
Northwestern Polytechnical University, Xi'an, 710072, P.R. China
xujin2njust@126.com

Abstract — This paper presents a novel dual-wideband bandpass filter (BPF) structure, which consists of a two-end shorted stepped-impedance resonator with two pairs of non-identical stepped-impedance open stubs (SIOSs) and a uniform-impedance open stub (UIOS) symmetrically loaded on its high impedance section. The designed BPF has a directly coupled configuration, which can also introduce transmission zero (TZ) for filter design. The loaded SIOSs and UIOS not only excite multiple resonant modes but also introduce multiple TZs. After carefully arranging these resonant modes and TZs, the TZs can divide multiple resonant modes into multiple useful groups, which can be utilized to exploit two wideband passbands. The TZs between two passbands can improve passband selectivity and the band-to-band isolation. As an example, a dual-wideband BPF centered at 1.57 / 5.59 GHz with -3 dB fractional bandwidth of 53% by 16% is designed and fabricated. The fabricated filter has a compact size of $0.16\lambda_g \times 0.106\lambda_g$. The measured results also exhibit a low insertion loss, good return loss and wide stopband.

Index Terms **-** Bandpass filter (BPF), dual-band, multiple- mode resonator (MMR), and stepped-impedance resonator (SIR).

I. INTRODUCTION

With the development of modern multi-service technology, dual-wideband bandpass filter (BPF) with compact size is great in demand for a single RF module to handle dual high data-rate communication modes. So far, various dual-band BPFs have been reported. However, most of these reported dual-band BPFs exhibit narrow passband [1-5]. One of the few literatures report the dual-wideband performance [6-9]. In [6], a dual-wideband BPF using frequency mapping and stepped-impedance resonators (SIRs) is reported, with the drawback of a complex design procedure and large circuit size. In [7], a dual-wideband BPF is developed by using the short-circuited SIRs, but it lacks passband selectivity. Two opposite hook-shaped resonators in [8] and four comb-loaded resonators in [9] are used to design the dual-wideband BPF. These two filters exhibit a high passband selectivity and compact size, but using multiple resonators. Recently, an attractive method using a single multiple-mode resonator (MMR) has been applied to develop compact dual-/multiple-band BPFs. Actually, MMR is widely used in the design of wideband filter [10-12]. Then, it is found that the multiple resonant modes of MMR can be arranged to be several mode groups in some structures, which can be applied to realize dual-/multiple-passband. In the author's previous work [13], two dual-mode, dual-wideband BPFs with sharp selectivity have been designed by using a quadruple-mode resonator. However, the etched ground plane configuration is involved, which increases the installation complexity.

The motivation of this paper is to design a novel microstrip dual-wideband BPF with single layer configuration, compact size, simple topology and quick design procedure. By properly arranging multiple resonant modes and multiple transmission zeros (TZs) of proposed structure, a dual-wideband BPF centered at 1.57 GHz / 5.59 GHz with -3 dB fractional bandwidth (FBW) of 53% by 16% are designed and fabricated. Detailed design of the filter as well as its simulated and measured results is presented and discussed.

Submitted On: May 12, 2013
Accepted On: Feb. 2, 2014

II. THEORETICAL ANALYSIS OF PROPOSED DUAL-BAND STRUCTURE

The configuration of the proposed dual-wideband BPF structure is shown in Fig. 1. Figure 2 (a) gives a transmission line model of the proposed structure. The proposed structure consists of a two-end shorted stepped-impedance resonator (SIR) with a pair of stepped-impedance open stubs (named SIOS1) loaded at the impedance junctions of the shorted SIR, the other pair of stepped-impedance open stubs (named SIOS2) symmetrically loaded on its Z_2-impedance section and a uniform impedance open stub (named UIOS) loaded at the center of Z_2-impedance section. The I/O ports are directly connected to the proposed structure. Due to its symmetrical configuration, Fig. 2 (b) and (c) give its even-/odd-mode equivalent circuits, respectively. The TPs can be derived under the transverse resonant condition that two oppositely oriented input impedances at the same position are zero. According to such theorem, the transmission poles (TPs) under the even-/odd-mode excitation satisfy,

$$\mathrm{Im}(Z_l + Z_{r,e}) = 0 \tag{1a}$$

$$\mathrm{Im}(Z_l + Z_{r,o}) = 0, \tag{1b}$$

where,

$$Z_l = Z_2[(jZ_{in\_SIOS1}Z_1\tan\theta_1 + jZ_2\tan(\theta_2/2 - \theta_{a1})(Z_{in\_SIOS1} + jZ_1\tan\theta_1)] / [Z_2(Z_{in\_SIOS1} + jZ_1\tan\theta_1) - Z_{in\_SIOS1}Z_1\tan\theta_1\tan(\theta_2/2 - \theta_{a1})] \tag{2a}$$

$$Z_{r,e} = Z_{in\_SIOS2}Z_2(2Z_{in\_UIOS} + jZ_2\tan\theta_{a1}) / [Z_{in\_SIOS2}(Z_2 + j2Z_{in\_UIOS}\tan\theta_{a1}) + Z_2(2Z_{in\_UIOS} + jZ_2\tan\theta_{a1})], \tag{2b}$$

$$Z_{r,o} = \frac{jZ_{in\_SIOS2}Z_2\tan\theta_{a1}}{Z_{in\_SIOS2} + jZ_2\tan\theta_{a1}}, \tag{2c}$$

$$Z_{in\_SIOS1} = jZ_{s11}\frac{Z_{s11}\tan\theta_{s11} - Z_{s12}\cot\theta_{s12}}{Z_{s11} + Z_{s12}\tan\theta_{s11}\cot\theta_{s12}}, \tag{2d}$$

$$Z_{in\_SIOS2} = jZ_{s21}\frac{Z_{s21}\tan\theta_{s21} - Z_{s22}\cot\theta_{s22}}{Z_{s21} + Z_{s22}\tan\theta_{s21}\cot\theta_{s22}}, \tag{2e}$$

$$Z_{in\_UIOS} = -jZ_u\cot\theta_u, \tag{2f}$$

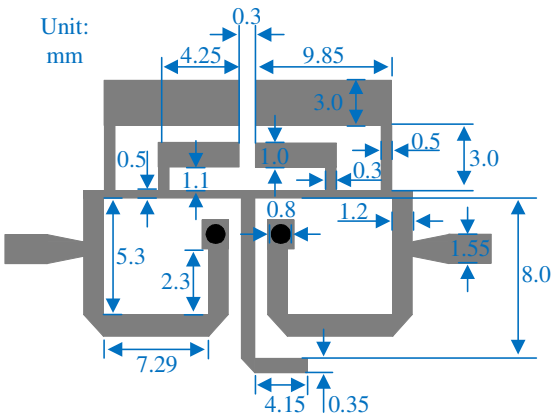

Fig. 1. Physical configuration of proposed dual-wideband BPF.

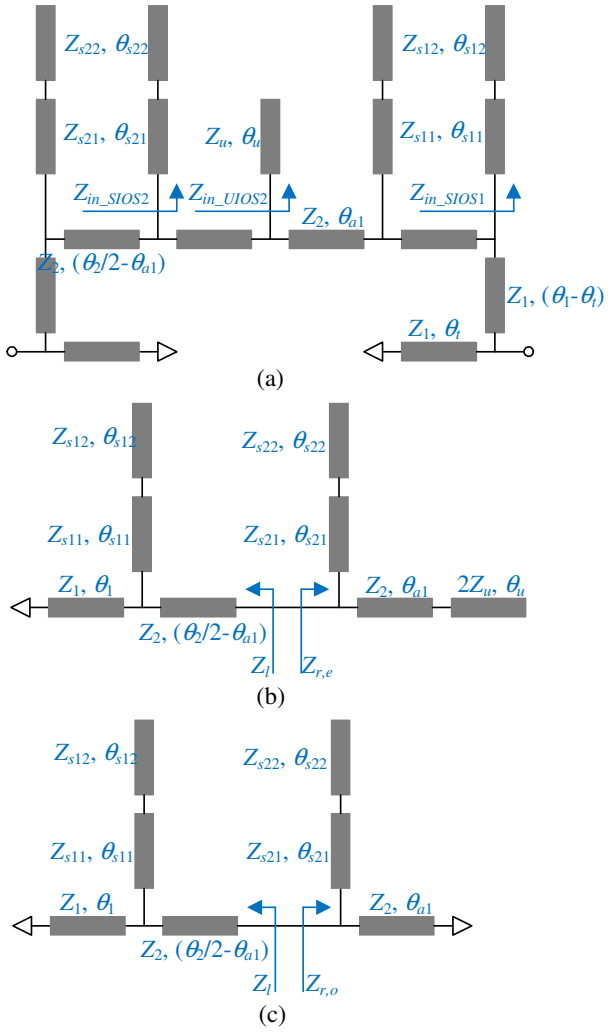

Fig. 2. (a) Transmission line model of proposed dual-wideband BPF, (b) even-mode equivalent circuit, and (c) odd-mode equivalent circuit.

If the input impedances of the SIOS1, SIOS2, and UIOS equal to zero, respectively, this is equivalent to introducing virtual grounds at the connected points. The signal from the input port will be shorted to ground and cannot transfer to the output port. Thus, the SIOS1, SIOS2, and UIOS will produce three series of TZs (f_{zs1}, f_{zs2}, and f_{zu}) for the proposed dual-wideband BPF structure. According to equations (2d), (2e), and (2f), these three series of TZs can be determined by,

$$Z_{s11}\tan\theta_{s11} - Z_{s12}\cot\theta_{s12} \quad (3a)$$

$$Z_{s21}\tan\theta_{s21} - Z_{s22}\cot\theta_{s22}, \quad (3b)$$

$$\cot\theta_u = 0. \quad (3c)$$

Equation (3c) can be rewritten as,

$$f_{zu} = \frac{n\pi f_0}{2\theta_u}, \quad n = 1, 3, 5\cdots \quad (4)$$

where f_0 represents the design frequency. Thus, f_{zu} can be separately controlled by θ_u. When θ_t equals to half-wavelength at f_{zt}, the input impedance looking into the tapped point will be also zero for directly coupled configuration, owing to the impedance invariance characteristic of half-wavelength line. Therefore, the feeding lines directly connected to the resonator not only act as I/O ports but also can produce a series of TZs. Such TZs due to the directly coupled configuration can be determined by,

$$f_{zt} = \frac{n\pi f_0}{\theta_t}, \quad n = 1, 2, 3\cdots \quad (5)$$

f_{zt} cannot be tunable freely, and the location of the tapped point θ_t is mainly determined by the required design condition. Subsequently, equations (1), (3a), (3b), (4), and (5) allow one to determine the frequency locations of all the even-/odd-mode TPs and TZs.

As an example, the central frequencies (CFs) of two passbands are specified at 1.575/5.5 GHz. There are various designing parameters that can be tuned to achieve such goal. The electrical length of shorted SIR ($2\theta_1+\theta_2$) is mainly decided by the specified f_0. In this design, ($2\theta_1+\theta_2$) = 150° at f_0 = 1.575 GHz is tuned to make the first mode group locate at around f_0. $\theta_1 = \theta_2$ is preset for the design simplicity. Z_1 is mainly determined by the required resonator susceptance and Z_1 = 58 Ω is preselected. SIOS1, SIOS2, UIOS, and the directly coupled configuration will generate four series of TZs. In the practical design, there are only four TZs (1^{st} f_{zs1}, 1^{st} f_{zs2}, 1^{st} f_{zu}, and 1^{st} f_{zt}) within the interested frequency range. It is found that the 1^{st} f_{zs1} and 1^{st} f_{zu} should be placed between two passbands. Since $\theta_{s12} = \theta_2/2$ is set for the following layout convenience, the frequency locations of the 1^{st} f_{zs1} are then tuned by $t_{s1} = \theta_{s11}/(2\theta_1+\theta_2)$ and $r_{s1} = Z_{s12}/Z_{s11}$. In this filter design, t_{s1} = 0.1 and $t_u = \theta_u/(2\theta_1+\theta_2)$ = 0.25 is pre-selected to make the 1^{st} f_{zs1} close to the lower side of the first passband and the 1^{st} f_{zu} close to the upper side of the second passband. The SIOS2 can be freely sliding on Z_2-impedance section. In this design, $\theta_{a1} = \theta_2/4$ is pre-selected for the design simplicity. Since $\theta_{s22} = \theta_{a1}$ is set for the following layout convenience, the frequency locations of the 1^{st} f_{zs2} are then tuned by $t_{s2} = \theta_{s21}/(2\theta_1+\theta_2)$ and $r_{s2} = Z_{s22}/Z_{s21}$. It is also found that the 1^{st} f_{zs2} should be placed between two passbands. Thus, t_{s2} = 0.02 is pre-selected. Due to the required external quality factor, the tapped position θ_t will be not very long, so that the 1^{st} f_{zt} together with 1^{st} f_{zs2} located beyond two passbands can extend the stopband. Under the remaining designing parameters at f_0 = 1.575 GHz selected as $r_{12} = Z_2/Z_1$ = 1.5, $r_u = Z_u/Z_1$ = 2, $r_{s11} = Z_{s11}/Z_1$ = 1.5, $r_{s12} = Z_{s12}/Z_{s11}$ = 0.35, $r_{s21} = Z_{s21}/Z_1$ = 2, $r_{s22} = Z_{s22}/Z_{s21}$ = 0.6, and t = 0.86, Fig. 3 gives a typically weak coupling frequency response of proposed structure. The 1^{st} f_{zs1} and the 1^{st} f_{zu} divide the first seven resonant modes into two groups, i.e., f_{pe1} and f_{po1} in the first mode group and f_{pe3}, f_{po2}, f_{pe4} and f_{po3} in the second passbands, which can be used to develop dual-band BPF. The TP f_{pe2} can be tuned to close to the 1^{st} f_{zs1}, so as to avoid forming the spurious passband.

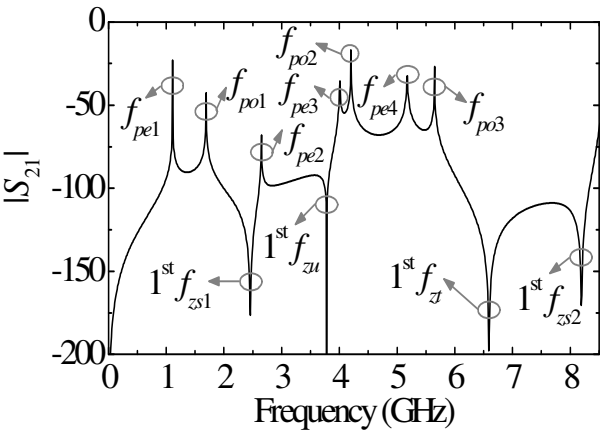

Fig. 3. Typically weak coupling frequency response of the proposed structure.

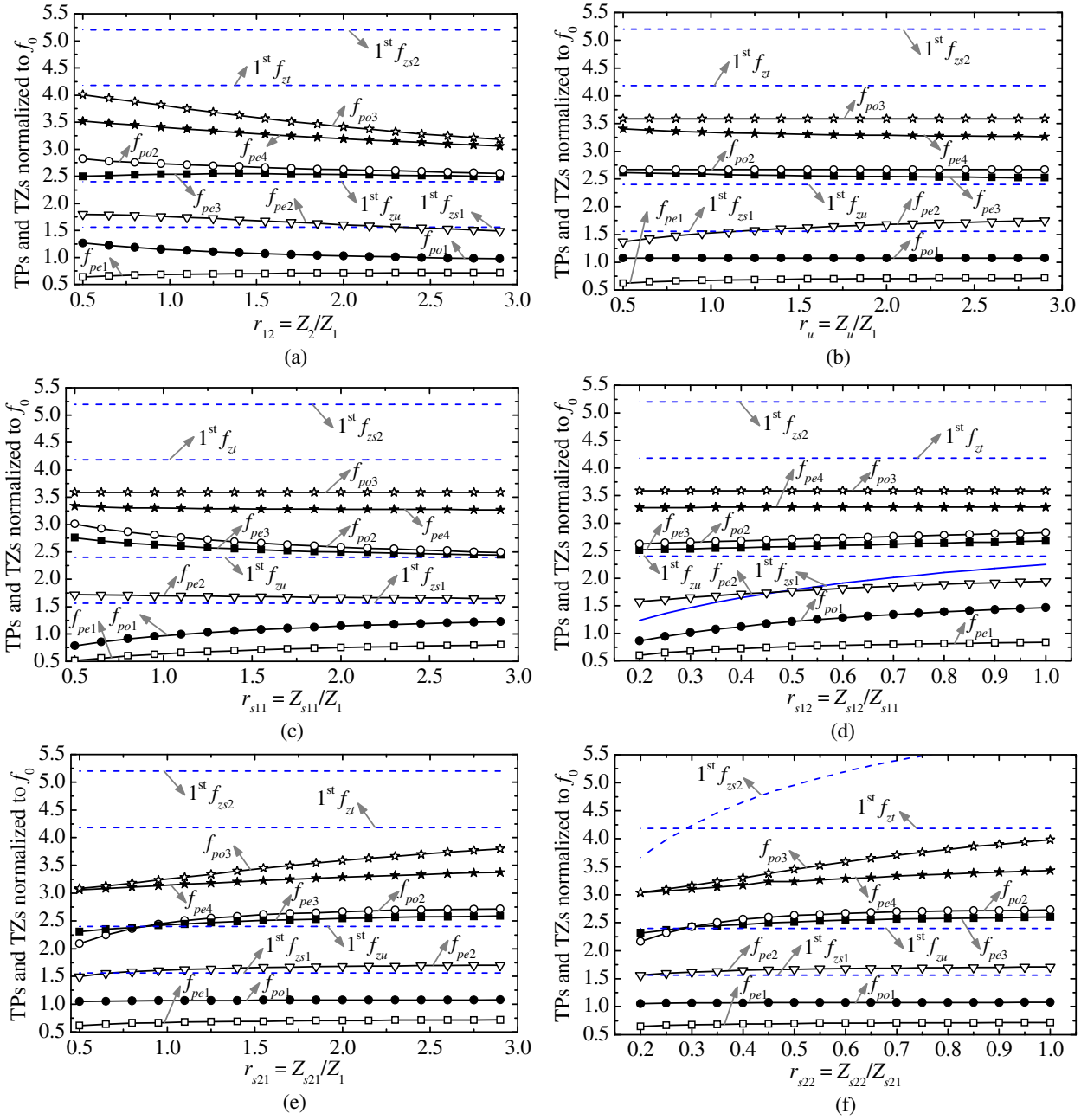

Fig. 4. Variation of TPs and TZs versus varied (a) r, (b) r_u, (c) r_{s11}, (d) r_{s12}, (e) r_{s21}, and (f) r_{s22}. When one designing parameter varies, the others keep in constant.

Based on the above discussion, the frequency locations of the resonant modes in each passband should be carefully tuned by r_{12}, r_u, r_{s11}, r_{s12}, r_{s21}, and r_{s22}, so as to achieve a good in-band performance of two passbands. Figure 4 gives the variation of all TPs and TZs versus varied r, r_{12}, r_u, r_{s11}, r_{s12}, r_{s21}, and r_{s22}. It can be seen in Fig. 4 (a) that as r increases, f_{po1} and f_{po3} move towards lower frequency while f_{pe1} and f_{pe3} do not shift dramatically. Since the above four TPs will mainly determine the bandwidths (BWs) and CFs of the two passbands, r should be firstly determined to acquire a roughly desired value of BWs and CFs of two passbands. To some extent, the BWs and CFs of the first passband can then be separately tuned by r_{s11} and r_{s12} as shown in Fig. 4 (c) and (d), while

the BWs and CFs of the second passband can be separately tuned by r_{s21} and r_{s22} as shown in Fig. 4 (e) and (f). It can be seen in Fig. 4 (d) that r_{s12} can be also used to tune the 1st f_{zs1} and f_{pe2} for achieving the goal of the free spurious-frequency isolation band. Thus, there is a tradeoff between such two purposes, when using r_{s12}. After the above five parameters are tuned to make the 1st f_{zs1} very close to f_{pe2}, r_u can be finally used to tune f_{pe2} for achieving the goal of the free spurious-frequency isolation band. Although the variation of r_u will affect the even-mode TPs, it can be seen in Fig. 4 (b) that all even-mode TPs except f_{pe2} do not change dramatically as it varies.

III. DUAL-WIDEBAND BPF DESIGN, SIMULATION, AND MEASURED RESULTS

Actually, it will be hard to directly find the final designing parameters, which can satisfy the desired in-band performance of two passbands and free spurious frequency isolation band simultaneously. So that the above initial designing parameters for dual-band BPF need to be optimized, which can be done with the help of ADS software. The designing parameters for dual-wideband BPF at f_0 = 1.575 GHz are optimized as Z_1 = 58 Ω, r_{12} = 1.6, $(2\theta_1 + \theta_2) = 144^o$, t_{12} = 0.31, r_u = 1.89, t_u = 0.23, r_{s11} = 1.6, r_{s12} = 0.34, t_{s1} = 0.07, r_{s21} = 2.22, r_{s22} = 0.59, t_{s2} = 0.022, and t_{s22} = 0.46. Under such designing parameters, two passbands of the filter are centered at 1.575 GHz / 5.435 GHz with -3dB fractional bandwidth of 57.8% by 20.7%, respectively. The filter is designed on ARlon DiClad 880 substrate (ε_{re} = 2.2, h = 0.508 mm). The whole structure is optimized by using the full-wave EM simulator HFSS and the optimized physical dimensions are labeled in Fig. 1. Figure 5 plots the external quality factor of two passbands against d_t. The external quality factor of the first passband (Q_{e1}) and the external quality factor of the second passband (Q_{e2}) are extracted by the following equation,

$$Q_{ex1,2} = \frac{f_{c1,2}}{\Delta_{1,2}} = \frac{f_{c1,2}}{\Delta_{(\pm\pi/2)1,2}} \tag{6}$$

where $\Delta_{1,2}$ and $\Delta f_{(\pm\pi/2)1,2}$ represents -3dB bandwidths and the frequency bandwidth of S_{11} phase curve changing $\pm\pi/2$ with respect to $f_{c1,2}$, respectively. As d_t increases, Q_{e1} slightly decreases while Q_{e2} apparently increases. The ascent rate of Q_{e2} is greater than the descent rate of Q_{e1}. In this paper, d_t = 15.765 is selected for two passbands. The overall circuit size is 22.38 mm × 14.85 mm, corresponding to $0.16\lambda_g \times 0.106\lambda_g$, where λ_g represents the guided wavelength of a 50 Ω microstrip line at 1.57 GHz. The photograph of the fabricated filter is shown in Fig. 6.

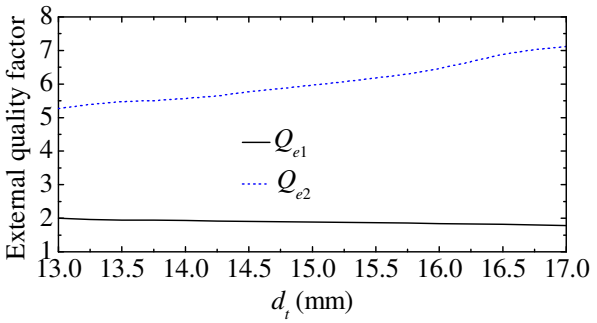

Fig. 5. External quality factor against d_t.

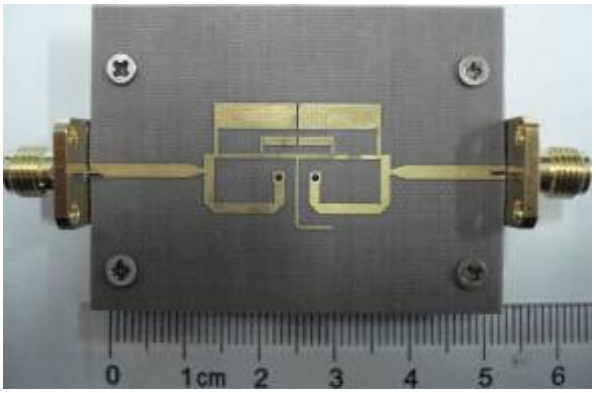

Fig. 6. Photograph of the fabricated dual-wideband BPF.

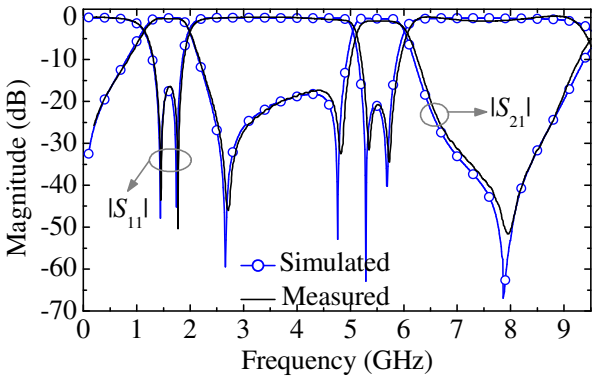

Fig. 7. Simulated and measured results of the fabricated dual-wideband BPF.

Table 1: Performance comparison with reported works.

	IL at CF(dB)/ -3 dB FBW	Roll of rate (dB/GHz)	Isolation (dB)	Circuit area (λ_g^2)
[6]	0.5/47.6%, 2/48.4%	33/200/80/100	> 40	3.33×1.08
[7]	0.8/54%, 0.8/20%	15/18/18/10	> 25	0.3×0.3
[8]	0.55/19.5%, 1.31/15.1%	99/75/87/56	> 13	0.065×0.147
[9]	1.1/32%, 2.5/13%	112/41/71/81	> 30	0.464×0.06
[13]	0.1/57.1%, 0.8/20.8%	63/45/71/50	> 30	0.40×0.05
This work	0.3/53%, 0.8/16%	22/39/74/35	> 17	0.16×0.106

The simulated and measured results of fabricated dual-band BPF are plotted in Fig. 7. Good agreement can be observed between the simulation and measurement results. There are some discrepancies, which are attributed to the fabrication error as well as the SMA connectors. The measured central frequencies (CFs) and -3 dB FBW of two passbands are 1.57 GHz / 5.59 GHz and 53% by 16%, respectively. The measured insertion losses (ILs) at two CFs are 0.3 dB / 0.8 dB while the return losses are better than 17 dB / 20 dB. There are only two TPs that can be observed in the second passband. This is because that f_{pe3} close to f_{po2} will merge into one poles, which is the same to f_{pe4} and f_{po3}. The band-to-band isolation is better than 17 dB from 2.3 GHz to 4.9 GHz. The fabricated filter also has -20 dB rejection level stopband from 6.5 GHz to 8.95 GHz. There is only one TZ within the stopband that can be observed in Fig. 7. This is because that the 1st f_{zt} will be very close to the 1st f_{zs2} after optimization. These two TZs merge into one TZ finally.

The comparison between the performances of some reported dual-wideband BPFs and the proposed one is summarized in Table 1. After comparison, it can be known that the proposed dual-wideband BPF in this paper has the merits of lower insertion losses, more compact size, and simpler physical topology.

IV. CONCLUSION

A dual-wideband BPF centered at 1.57 GHz / 5.59 GHz with -3 dB FBW of 53% by 16 % and compact size of $0.16\lambda_g \times 0.106\lambda_g$ are presented in this paper. Measured results also show its merits of low insertion loss, good return loss, sharp passband selectivity, and good band-to-band isolation. The proposed filter has simple topology and design procedure. All these merits make it attractive in modern dual high data-rate communication system.

REFERENCES

[1] M. Hayati, A. Khajavi, and H. Abdi, "A Miniaturized microstrip dual-band bandpass filter using folded UIR for multimode WLANs," *Applied Computational Electromagnetics Society (ACES) Journal*, vol. 28, no. 1, pp. 35-40, January 2013.

[2] S. Sun, "A dual-band bandpass filter using a single dual-mode ring resonator," *IEEE Microw. Wireless Compon. Lett.*, vol. 21, no. 6 pp. 298-300, 2011.

[3] Y. Sung, "Dual-mode dual-band filter with band notch structures," *IEEE Microw. Wireless Compon. Lett.*, vol. 20, no. 2, pp. 73-75, 2011.

[4] J. Xu, C. Miao, and W. Wu, "A compact and high isolation dual-mode dual-band bandpass filter with tunable transmission zeros," *J. of Electromag. Waves and Appl.*, vol. 26, no. 17-18, pp. 2390-2397, 2012.

[5] X. Li and J. Zeng, "A novel dual-band microstrip bandpass filter design and harmonic suppression," *Applied Computational Electromagnetics Society (ACES) Journal*, vol. 28, no. 4, pp. 348-352, April 2013.

[6] A.-S. Liu, T.-Y. Huang, and R.-B. Wu, "A dual-wideband filter design using frequency mapping and stepped-impedance resonators," *IEEE Trans. Microw. Theory Tech.*, vol. 56, no. 12, pp. 2921-2929, 2008.

[7] K.-S. Chin and J.-H. Yeh, "Dual-wideband bandpass filter using short-circuited stepped-impedance resonators," *IEEE Microw. Wireless Compon. Lett.*, vol. 19, no. 3 pp. 155-157, 2009.

[8] Z. Zhang, Y.-C. Jiao, X.-M. Wang, and S.-F. Cao, "Design of a compact dual-band bandpass filter using opposite hook-shaped resonator," *IEEE Microw. Wireless Compon. Lett.*, vol. 21, no. 7 pp. 359-361, 2011.

[9] C.-W. Tang and Y. Hsu, "Design of wide-single-/dual-passband filters with comb-loaded resonators," *IET Microw. Antennas Progap.*, vol. 6, no. 1 pp. 10-16, 2012.

[10] C. Liu, T. Jiang, Y. Li, and J. Zhang, "A novel UWB filter with WLAN and RFID stop-band rejection characteristics using tri-stage radial loaded stub resonators," *Applied Computational Electromagnetics Society (ACES) Journal*, vol. 27, no. 9, pp. 749-758, Sep. 2012.

[11] S. Gao, S. Xiao, and J.-L. Li, "Compact ultra-wideband (UWB) bandpass filter with dual notched bands," *Applied Computational Electromagnetics Society (ACES) Journal*, vol. 27, no. 10, pp. 795-800, Oct. 2012.

[12] Y. Li, H. Yang, Y. Wang, and S. Xiao, "Ultra-wideband bandpass filter based on parallel-coupled microstrip lines and defected ground structure," *Applied Computational Electromagnetics Society (ACES) Journal*, vol. 28, no. 1, pp. 21-26, Jan. 2013.

[13] J. Xu, W. Wu, and C. Miao, "Compact and sharp skirts microstrip dual-mode dual-band bandpass filter using a single quadruple-mode resonator (QMR)," *IEEE Trans. Microw. Theory Tech.*, vol. 61, no. 3, pp. 1104-1113, 2013.

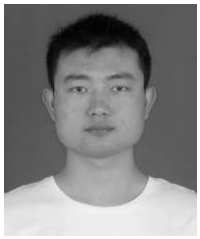

Jin Xu was born in AnHui, China, in 1987. He received the B.Eng. degree in Information Countermeasure Technology and Ph.D. degree in Information and Communication Engineering from Nanjing University of Science and Technology (NUST), Nanjing, China, in 2009 and 2013, respectively. He is currently an Associate Professor with the College of Electronic Information, Northwestern Polytechnical University, Xi'an, China. His research interests include UWB technology, MCM technology, microwave passive/active components, microwave and millimeter-wave MMICs developed on SiGe, phased array radar and wireless communication system.

From February 2011 to September 2011, he was an attached Ph.D. student in Institute of Microelectronics, Singapore. From October 2011 to September 2012, he joined MicroArray Technologies Corporation Limited, Chengdu, P.R. China, where he was an IC R&D Engineer. Since 2011, he has served as a reviewer for some journals including IEEE Microwave Wireless Component Letters, International Journal of Electronics, PIER and JEMWA.